Electrochimica Acta 55 (2010) 5258–5262

Contents lists available at ScienceDirect

Electrochimica Acta

journal homepage: www.elsevier.com/locate/electacta

Preparation and electrochemistry of NiO/SiNW nanocomposite electrodes for electrochemical capacitors

Bairui Tao [a,b], Jian Zhang [b,*], Fengjuan Miao [a,b], Shichao Hui [b], LiJuan Wan [b]

[a] College of Communications and Electronics Engineering, Qiqihar University, 42 Wenhua Street, Qiqihar, Heilongjiang 161006, China
[b] Key Laboratory of Poling Materials and Devices of MOE and State Key Laboratory of Transducer Technology, East China Normal University, 500 Dong Chuan Road, Shanghai 200241, China

ARTICLE INFO

Article history:
Received 12 January 2010
Received in revised form 13 April 2010
Accepted 15 April 2010
Available online 21 April 2010

Keywords:
Electrochemical capacitor properties
NiO/Si nanowire composites
Electroless plating

ABSTRACT

This paper studies nickel oxide/silicon nanowires (NiO/SiNWs) as composite thin films in electrodes for electrochemical capacitors. The SiNWs as backbones were first prepared by chemical etching, and then the Ni/SiNW composite structure was obtained by electroless plating of nickel onto the surface of the SiNWs. Next, the NiO/SiNW nanocomposites were fabricated by annealing Ni/SiNW composites at different temperatures in an oxygen atmosphere. Once the electrodes were constructed, the electrochemical behavior of these electrodes was investigated with cyclic voltammetry (CV) and electrochemical impedance spectroscopy (EIS). In 2 M KOH solution, the electrode material was found to have novel capacitive characteristics. Finally, when the NiO/SiNW composites were annealed at 400 °C, the maximum specific capacitance value was found to be as high as 681 F g^{-1} (or 183 F cm^{-3}), and the probing of the cycling life indicated that only about 3% of the capacity was lost after 1000 charge/discharge cycles. This study demonstrated that NiO/SiNW composites were the optimal electrode choice for electrochemical capacitors.

© 2010 Elsevier Ltd. All rights reserved.

1. Introduction

Electrochemical capacitors are considered one of the potential systems for energy storage, in addition to batteries and fuel cells. There are two types of electrochemical capacitors based on the types of electrochemical response: electrical double layer (EDL) capacitors and pseudocapacitors [1–3]. With the advent of nanotechnology, nanomaterials with high surface area and fast redox reactions have been realized. Consequently, it has been possible to generate appropriate nanostructured electrode materials with good capacitance characteristics [4]. Among the several transition metal oxides studied for capacitor response to date, ruthenium oxide has been widely researched and known for its superior electrochemical capacitor response [5]. Unfortunately, the expensive nature of ruthenium has limited the technological viability of this material. Finding low-cost transition metal oxides that are compatible with current IC processes as electrode materials for integrated electrochemical capacitors is a big challenge in this field.

Among the candidates for electrode materials, nanoscale or nanocomposite materials based on nickel oxide (NiO) [6–8], manganese oxide (MnO_2) [9–12] and cobalt oxide (CoO_x) [13,14] were prepared for the fabrication of electrochemical capacitors. Nickel oxide, with a stable band gap of 3.25–4.0 eV, has been considered one of the most promising potential electrode materials for electrochemical capacitors [15–18]. Electrochemical capacitors constructed of composites fabricated from nickel oxide/carbon nanotubes (NiO/CNTs) have been reported with specific capacity values of 160 F g^{-1}, 384 F g^{-1} and 457.63 F g^{-1} [19–21]. Although these NiO/CNT nanocomposite structures could significantly improve the electrical conductivity of the host NiO by increasing the number of active sites for the redox reaction of the metal oxide, the complete process is complicated. In addition to the fabrication process not being compatible with current IC processes, this complexity will impede its application in micro- and nano-devices.

Therefore, nickel oxide/silicon nanowire (NiO/SiNW) nanocomposites as electrochemical capacitor electrodes are proposed in this study. The NiO/SiNW nanocomposites exhibiting high surface-to-volume area and surface activity were fabricated as working electrodes to measure their electrochemical capacitor performance by cyclic voltammetry (CV), galvanostatic charge/discharge and electrochemical impedance spectroscopy (EIS).

2. Experimental

2.1. Raw materials

Single-polished N-type heavily Sb-doped silicon wafers with ⟨1 0 0⟩-orientation and resistivity of 0.01–0.05 Ω cm were used as the substrates for SiNW growth. $AgNO_3$, $NiSO_4{\cdot}6H_2O$, $(NH_4)_2SO_4$,

* Corresponding author. Tel.: +86 21 54345203; fax: +86 21 54345119.
E-mail addresses: jzhang@ee.ecnu.edu.cn, tbr_sir@163.com (J. Zhang).

0013-4686/$ – see front matter © 2010 Elsevier Ltd. All rights reserved.
doi:10.1016/j.electacta.2010.04.057

Table 1
Materials and conditions used in the electroless nickel plating process.

Chemical	Concentration (M)	Function
$NiSO_4{\cdot}6H_2O$	1	Ni source
$(NH_4)_2SO_4$	0.5	Buffering agent
Sodium dodecyl sulfate	0.001	Surfactant
NH_4F	2.5	Reductant
Sodium succinate	0.2	Accelerant
Sodium citrate	0.2	Chelating agent
Ammonia	X	Adjust pH 8.5–9.5

NH_4F, hydrofluoric acid, sodium dodecyl sulfate, sodium succinate, sodium citrate and ammonia were all analytical reagents. All chemicals were used as received without further purification.

2.2. Formation of the SiNWs

The SiNWs were first fabricated by wet chemical etching with an etchant of $AgNO_3$ (25 mM) to HF (15%) in a 1:1 volume ratio. The cleaned silicon chips were etched for 40 min with 200 mL of etchant in polytetrafluoroethylene containers at room temperature. The detailed process for SiNW preparation can be found elsewhere [22]. Next, all chips were taken out from the solution and rinsed with DI water and diluted nitric acid (~30%) in order to remove the residue on the surface of the silicon nanowires. After careful drying, the mass of the 12 chips was weighed with an ultra-microbalance with a mass resolution of 0.001 mg (Mettler Toledo, Switzerland).

2.3. Fabrication of NiO/SiNW nanocomposites

Ni/SiNW nanocomposites were obtained by electroless nickel plating onto the SiNW backbone [23]. First, the fabricated SiNWs were put into a buffer solution (Triton X-100) for 30 s to enhance wetting and then immersed in the plating bath for 360 s. Afterwards, they were removed and rinsed with DI water. The materials and conditions used in the electroless nickel plating process are listed in Table 1. The mass of the received Ni/SiNW nanocomposite chips was weighed and recorded.

Next, 12 Ni/SiNW nanocomposite chips were divided into three groups, labeled as Group A to Group C, with each group containing four chips. Chips of Group A to Group C were annealed for 600 s at 300 °C, 400 °C and 500 °C, respectively, using a rapid annealing system with an O_2 flow rate of 120 mL min^{-1}. The masses of the resulting nanocomposites were also weighed and recorded.

The NiO/SiNW chips obtained were used for both material characterization and electrochemical capacitor electrode development.

2.4. Electrochemical analysis of NiO/SiNW nanocomposites

The electrochemical properties of the NiO/SiNW nanocomposites as working electrodes in 2 M KOH aqueous solution were characterized. The electrodes were constructed by gluing a copper leading wire onto the NiO/SiNW nanocomposite chips, which had an area of approximately 1 cm^2. Cyclic voltammetry (CV), electrochemical impedance spectroscopy (EIS) and charge–discharge testing were performed using an electrochemical workstation (LK3200A, Lanlike, China) with a platinum foil counter electrode and a saturated Ag/AgCl reference electrode.

3. Results and discussion

3.1. Characterization of NiO/SiNW nanocomposites

It has been reported that Ni films will oxidize when the annealing temperature is over 300 °C [23,24]. After the annealing process in our study, therefore, the Ni/SiNW nanocomposites will turn into NiO_x/SiNW nanocomposites.

Fig. 1(a and b) shows the top-view and close-up view of scanning electron microscopy (SEM) images, respectively, for the resulting Ni/SiNW nanocomposites. It can be seen that SiNWs formed bundle-like structures with an additional layer plated onto the SiNW surface. The overall length of the Ni/SiNWs was found to be ~20 μm, and the diameters ranged from 60 nm to 400 nm. Both the length and the width of the SiNWs could be controlled by adjusting the etching time, the recipe of etchant and the temperature for SiNW fabrication [25].

Fig. 2(a, b, and c) shows the top-view SEM images of samples A, B, and C, respectively. It can be seen from these figures that the spongy and folded surface structure was observed in samples A and B but that nickel oxide particles agglomerated in sample C.

The energy dispersive spectrum (EDS) analysis results of sample B are shown in Fig. 3. This analysis verified that only the peaks corresponding to Ni and O could be found for the prepared NiO/SiNW nanocomposites. All of the recorded EDS spectra for other samples were similar to that shown in Fig. 3. For all the received nanocomposites, only the characteristic peaks of Ni and O were found in the EDS spectra, indicating that nickel oxides formed in the nickel layer. No characteristic peaks corresponding to Si were found, however, implying that the nickel oxide coating is formed as a dense layer. In addition, EDS analysis indicated that the oxygen content increased from samples A to C with increasing annealing temperature.

The mass differences before and after Ni/SiNW nanocomposite oxidation also confirmed the formation of a NiO_x layer. By measuring the mass changes before and after Ni/SiNW nanocomposite oxidation, the mass of oxygen incorporated into composite was

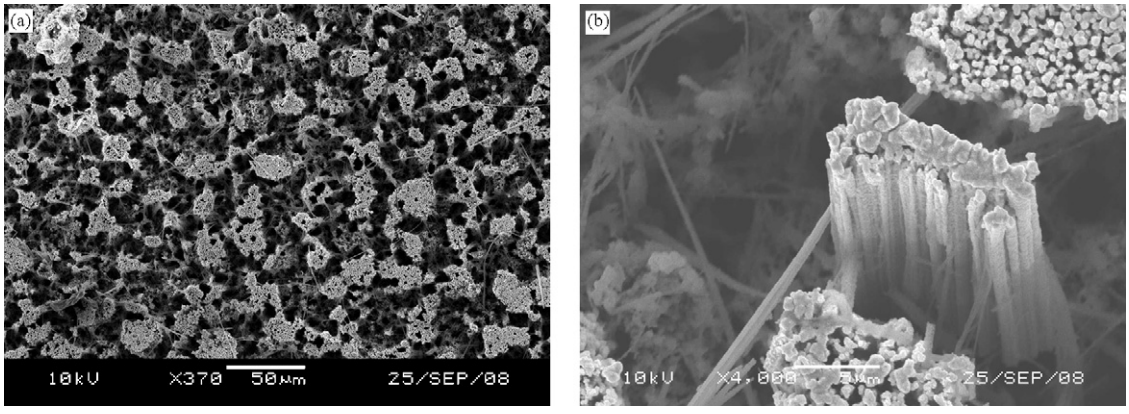

Fig. 1. SEM images of Ni/SiNWs: (a) top view and (b) close-up view.

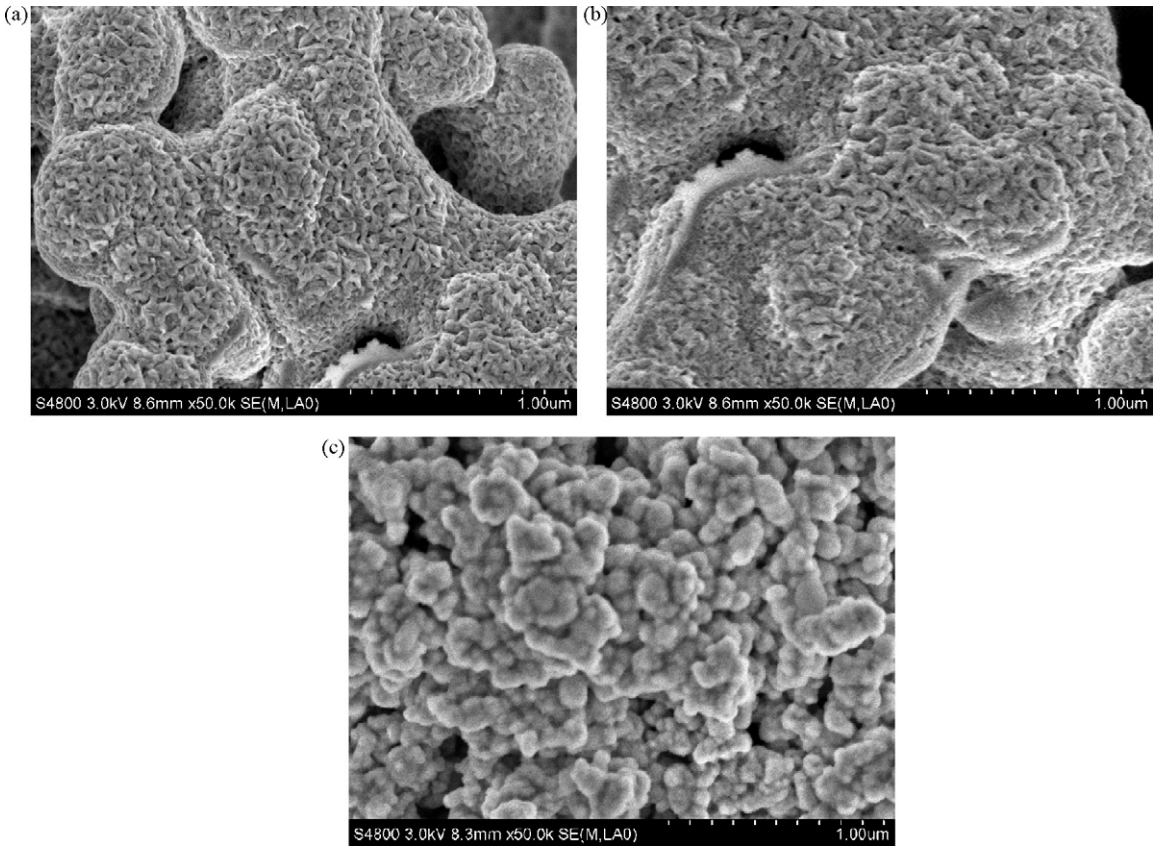

Fig. 2. Top-view SEM micrograph of NiO/SiNWs: (a) annealed at 300 °C, (b) annealed at 400 °C and (c) annealed at 500 °C.

measured. The maximum mass of NiO on each chip (annealed at 300 °C, 400 °C and 500 °C) was then estimated as 0.122 mg, 0.583 mg and 0.685 mg, respectively, if we assumed that only NiO was formed during the oxidation.

3.2. Electrochemical capacitive behavior of NiO/SiNW electrodes

Fig. 4(a, b, and c) shows the CV curves for the electrochemical capacitance of samples A, B and C in the potential range of −0.9 V to −0.4 V vs. Ag/AgCl with scan rates of 5 mV s^{-1}, 10 mV s^{-1} and 20 mV s^{-1}, respectively. For all samples, the pseudocapacitance effect could be observed, since both oxidation and reduction peaks occurred. Across the different annealing temperatures, the CV curves showed little difference. For samples A, B and C annealed at 300 °C, 400 °C and 500 °C, respectively, the double layer capacitance covered the potential range from −0.9 V to −0.55 V, and both the double layer capacitance and the pseudocapacitance occurred in the potential range of −0.55 V to −0.4 V during the anodic process at a scan rate of 5 mV s^{-1}. The distance between oxidation and reduction peak potentials of each sample became larger, and the reduction peak potentials shifted to the left side of the spectrum with increasing scan rate and annealing temperature. Among the samples, sample B showed the biggest oxidation and reduction peak current with the ideal rectangular shape for CV curves.

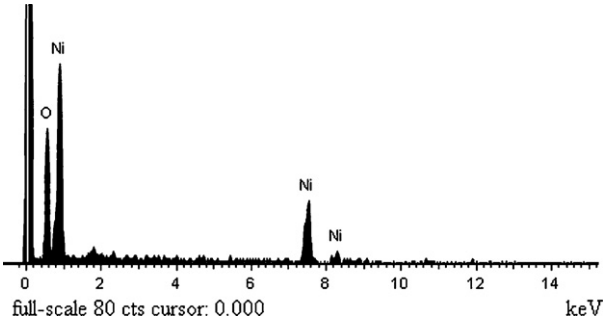

Fig. 3. Energy dispersive spectrum of NiO/SiNWs.

In all cases, the maximum peak potential difference (ΔE_p) between cathode reduction peak potential (E_{pc}) and anodic oxidation peak potential (E_{pa}) was about 260 mV, and the ratio of peak current (I_{pr}), the anodic oxidation peak current (I_{pc}) and cathode reduction peak current (I_{pa}) was close to 1. This observation indicated that the redox reaction was a quasi-reversible process.

The capacitance was estimated by the formula $C = \int idu/\Delta Uv$, where i is the real time current of CV, ΔU is the difference between initial potential and switching potential, t is the scan time, $v = du/dt$ is the scan rate and du is the difference in scan voltage. Therefore, the capacitance was related to the anodic oxidation process, C_a, and the cathodic reduction process, C_c, could therefore be estimated from the integral area of the CV curve bounded by the area of the oxidation and reduction peaks.

The results of C_a and C_c at different conditions are listed in Table 2. From these data, it was further demonstrated that the redox reaction was a quasi-reversible process due to the almost equivalent values of C_a and C_c for each electrode. The maximum electrochemical capacitance value was ~360 mF in a 1 cm^2 geometrical surface area of sample B at a scan rate of 5 mV s^{-1} in 2 M KOH solution, which was 1.8×10^5 times larger than the typical value of an electrical double layer capacitance (20 μF cm^{-2} [26]), implying that the Faradic reaction dominated the process.

The electrochemically active area (S_{ea}, cm^2), the mass specific capacitance (C_{ms}, F g^{-1}) and the capacitance density (C_{ds},

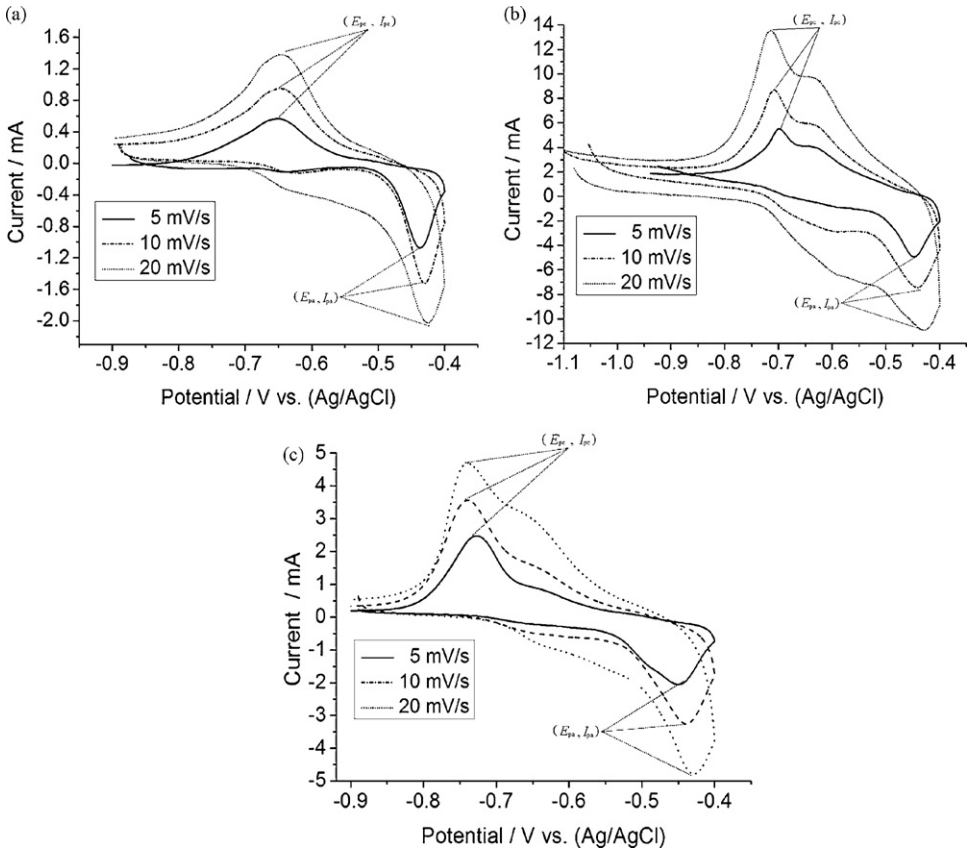

Fig. 4. Cyclic voltammetric evolutions of the electrodes: (a) annealed at 300 °C, (b) annealed at 400 °C and (c) annealed at 500 °C.

Table 2
Electrochemical information for the electrodes from CV at different scan rates.

Scan rate (mV s^{-1})	Sample A				Sample B				Sample C			
	C_a (mF)	C_c (mF)	ΔE_p (mV)	I_{pr}	C_a (mF)	C_c (mF)	ΔE_p (mV)	I_{pr}	C_a (mF)	C_c (mF)	ΔE_p (mV)	I_{pr}
5	30.4	30.1	214.4	1.35	360.5	373.3	239.4	0.96	226.4	246.4	256	0.86
10	19.7	22.3	218.5	1.31	344.8	365.8	248.3	0.90	181.6	192.4	263	0.91
20	17.6	16.3	221.9	1.21	277.6	290.1	256.6	0.89	141.1	151.2	277	1.01

F cm^{-3}) of the NiO/SiNW composites in each electrode were also estimated in this study. The results were calculated from the formula $S_{ea} = Q/210\ \mu C\ cm^{-2}$, where 210 μC cm^{-2} was assumed as the charge/cm^2 of the reference to Pt with a monolayer adsorption of hydrogen, and they are summarized in Table 3 [27].

For sample B, the values of S_{ea}, C_{ms} and C_{ds} were 888.7 cm^{-2}, 681.04 F g^{-1} and 183.2 F cm^{-3}, respectively, at a scan rate of 5 mV s^{-1}.

The above-mentioned results indicated that the capacitance of NiO/SiNW nanocomposite electrodes could be chiefly attributed to pseudocapacitance, which was caused by nickel undergoing a series of redox reactions and resulting in the formation of reversible hydroxides on its surface. This quasi-reversible pseudocapacitance redox reaction of NiO on electrodes in alkaline solution could be expressed as [28]:

$$NiO + OH^- \leftrightarrow NiOOH + e^- \quad (1)$$

Table 3
Electrochemical parameters of the electrodes in 2 M KOH solution at the scan rate of 5 mV s^{-1} by cyclic voltammetry.

	Q (C)	S_{ea} (cm^2 g^{-1})	m (mg)	C_{ms} (F g^{-1})	C_{ds} (F cm^{-3})
Sample A	0.015	5.91×10^5	0.122	247.95	15.2
Sample B	0.184	1.65×10^6	0.538	681.04	183.2
Sample C	0.118	8.56×10^5	0.685	345.11	118.2

3.3. Galvanostatic charge/discharge analysis

Fig. 5 shows the galvanostatic charge/discharge curves of sample B measured in 2 M KOH solution at galvanostatic currents of 5 mA and 2 mA. The charging time from 0 V to ~0.58 V was found

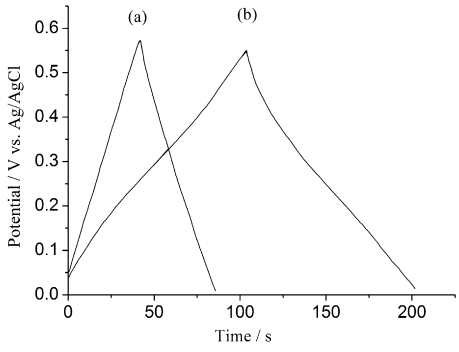

Fig. 5. Galvanostatic charge/discharge curves: (a) at 5 mA and (b) at 2 mA.

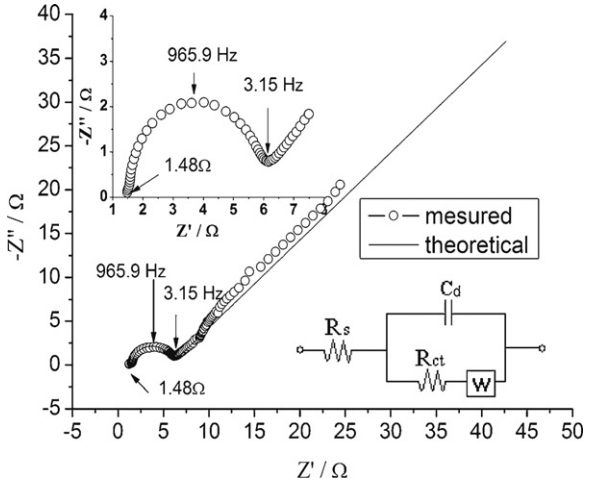

Fig. 6. Electrochemical impedance spectroscopy of sample B.

to be slightly longer than the discharging time from ~0.58 V to 0 V. Similar time lengths for charging and discharging implied that a reversible Faraday reaction took place on the active surface of the nickel oxide. After 1000 charge/discharge cycles, the specific capacitance value of 660.2 F g^{-1} was retained, and only ~3% of the capacitance was found to be lost. This phenomenon indicated that the NiO/SiNW electrodes had excellent charge/discharge stability.

3.4. Electrochemical impedance spectroscopy

To study the electrochemical response of the NiO/SiNW nanocomposite electrodes, electrochemical impedance spectroscopy (EIS) was performed with a frequency range of 10^5 Hz to 10^{-1} Hz and an AC perturbation amplitude of 10 mV. The complex Nyquist diagrams for sample B measured in 2 M KOH solution are shown in Fig. 6. The fitting curve, followed by Randles equivalent circuit, was also obtained and shown in the bottom right of Fig. 6. Two distinct, semi-circular regions were found in the high-frequency region, and an approximately straight line was observed in the low-frequency region. For high frequency ($\omega \to \infty$), an equivalent internal resistance, R_s, of ~1.5 Ω could be obtained, which included the ohmic resistance of the electrolyte and the particle contact resistance between the electrode material and the electrolyte interface. Additionally, the charge transfer resistance, R_{ct}, of ~4.5 Ω could be estimated by the diameter of the quarter-distorted circle in the inset of Fig. 6. Under 3.15 Hz, the impedance plot exhibited an approximately straight line, indicating a Warburg region, which attributed to the diffusion transfer limitation of charged ions in the presence of aggregated NiO nanoparticles [29].

So far, the NiO/SiNW nanocomposites proposed have been demonstrated to be potential electrode materials for electrochemical capacitors. The large surface-to-volume ratio was cited as an excellent reason to employ the silicon nanowire structure as the backbone for Ni deposition. Additionally, the particle-like or sponge-like character of the Ni increased the surface area further. The SiNWs fabricated from heavily Sb-doped silicon wafers with Ni electroless plating films could also be used simultaneously as current collectors. The internal resistance, R_s, of the electrochemical capacitor could be decreased by either optimizing the conductivity of the NiO/SiNW composite structure or choosing the higher conductivity substrate, silicon. Furthermore, the nickel silicide layers at the interface of the SiNWs and Ni, which showed resistance to OH^- etching and led to the superior redox cycling stability of the material, could form at an annealing temperature of 400 °C [30].

4. Conclusion

The NiO/SiNW nanocomposite electrodes exhibited excellent electrochemical performance in the form of high capacitance, long redox cycling life and quasi-reversible faradaic redox reactions for electrochemical capacitors. Therefore, the NiO/SiNW nanocomposites would be one of the optimal electrode materials for integrated electrochemical capacitors.

Acknowledgements

The National Natural Science Foundation of China (Grant No. 60672002) is gratefully acknowledged, as well as the Innovation Program of Shanghai Municipal Education Commission (Grant No. 09ZZ46). We are grateful for their financial support.

References

[1] P. Lunkenheimer, A. Loidl, C.R. Ottermann, K. Bange, Phys. Rev. B 44 (1991) 5927.
[2] T. Kim, Y.H. Mo, K.S. Nahm, S.M. Oh, J. Power Sources 162 (2006) 1275.
[3] K.W. Leitner, M. Winter, J.O. Besenhard, J. Solid State Electrochem. 8 (2003) 15.
[4] I. Hotovy, J. Huran, L. Spiess, S. Hascik, V. Rehacek, Sens. Actuators B 57 (1999) 147.
[5] S. Ohara, J. Suzuki, K. Sekine, T. Takamura, J. Power Sources 136 (2004) 303.
[6] S. Maensiri, P. Thongbai, T. Yamwong, Acta Mater. 55 (2007) 2851.
[7] P. Tomczyk, G. Mordarski, J. Oblakowski, J. Electroanal. Chem. 353 (1993) 177.
[8] C.Z. Yuan, L.H. Su, B. Gao, X.G. Zhang, Electrochim. Acta 53 (2008) 7039.
[9] C.J. Xu, B.H. Li, H.D. Du, F.Y. Kang, Y.Q. Zeng, J. Power Sources 184 (2008) 691.
[10] Y.C. Hsieh, K.T. Lee, Y.P. Lin, N.L. Wu, S.W. Donne, J. Power Sources 177 (2008) 660.
[11] R.C. Makkus, K. Hemmes, J.H.W. de Wit, J. Electrochem. Soc. 141 (1994) 3429.
[12] R.K. Sharma, A.C. Rastogi, S.B. Desu, Electrochim. Acta 53 (2008) 7690.
[13] G.C. Silva, C.S. Fugivara, G. Tremiliosi Filho, P.T.A. Sumodjo, A.V. Benedetti, Electrochim. Acta 47 (2002) 1875.
[14] A. Salimi, R. Hallaj, H. Mamkhezri, S.M.T. Hosaini, J. Electroanal. Chem. 31 (2008) 619.
[15] A. Salimi, R. Hallaj, H. Mamkhezri, S.M.T. Hosaini, J. Alloys Compd. 462 (2008) 356.
[16] G. Boschloo, A. Hagfeldt, J. Phys. Chem. B 105 (2001) 3039.
[17] A.J. Varkey, A.F. Fort, Thin Solid Films 235 (1993) 257.
[18] U.M. Patil, R.R. Salunkhe, K.V. Gurav, C.D. Lokhande, Appl. Surf. Sci. 255 (2008) 2603.
[19] J.Y. Lee, K. Liang, K.H. An, Y.H. Lee, Synth. Met. 150 (2005) 153.
[20] B. Gao, C.Z. Yuan, L.H. Su, S.Y. Chen, X.G. Zhang, Electrochim. Acta 54 (2009) 3561.
[21] S.H. Yan, P. Qu, H.T. Wang, T. Tian, Z.D. Xiao, Mater. Res. Bull. 43 (2008) 2818.
[22] L.J. Wan, W.L. Gong, K.W. Jiang, H.L. Li, B.R. Tao, J. Zhang, Appl. Surf. Sci. 254 (2008) 4899.
[23] B.R. Tao, J. Zhang, F.J. Miao, H.L. Li, L.J. Wan, Y.T. Wang, Sens. Actuators B 136 (2009) 144.
[24] S.J. Geng, F.H. Wang, S. Zhang, Surf. Coat. Technol. 167 (2003) 212.
[25] M.L. Zhang, K.Q. Peng, X. Fan, J.S. Jie, R.Q. Zhang, S.T. Lee, N.B. Wong, J. Phys. Chem. C 112 (2008) 4444.
[26] T. Pajkossy, D.M. Kolb, Electrochim. Acta 53 (2008) 7403.
[27] T. Morimoto, K. Hiratsuka, Y. Sanada, K. Kurihara, J. Power Sources 60 (1996) 239.
[28] M.Q. Wu, J.H. Gao, S.R. Zhang, C. Ai, J. Power Sources 159 (2006) 365.
[29] A.S. Adekunle, K.I. Ozoemena, Electrochim. Acta 53 (2008) 5774.
[30] M. Bhaskaran, S. Sriram, L.W. Sim, J. Micromech. Microeng. 18 (2008) 095002.